Deriving the Dynamical Motion of a Spinning Magnetic Dipole in External Magnetic and Gravitational Fields: Theory and Implications of Field Reversal

Joseph Havens[1] and Lucciana M. Caceres Holgado[1]

[1]*Department of Physics and Astronomy, University of Kansas, Lawrence, KS 66045, USA*

ABSTRACT

We present a detailed derivation and analysis of the rotational dynamics of a rigid, symmetric body possessing a magnetic dipole moment (μ) and subject to both an external uniform magnetic field (B) and a uniform gravitational field (g). Utilizing the Euler angle formalism (ϕ, θ, ψ) and Lagrangian mechanics, we derive the equations of motion that govern the system's precession, nutation, and spin. The principal moments of inertia are $I_1 = I_2$ and I_3, and the center of mass is a distance l from the pivot. The response of the system to a reversal of the external magnetic field is analyzed, considering the interplay between magnetic and gravitational torques. This model is applied to phenomena analogous to those observed in the TeachSpin Magnetic Torque experiment. We investigate how the precession direction is affected by magnetic field inversion, even with constant spin, and explore the conditions under which such changes occur. The role of conserved quantities and the conditions for steady precession are discussed.

1. INTRODUCTION

The interaction of rotating magnetic dipoles with external fields is a cornerstone problem in classical physics, bridging the disciplines of electromagnetism and analytical mechanics. Its manifestations are diverse, ranging from the behavior of spinning celestial bodies with magnetic fields to the principles underlying magnetic resonance phenomena. The TeachSpin Magnetic Torque apparatus provides an elegant and tangible demonstration of these principles, typically showcasing a cue ball with an embedded magnet. When spun and subjected to an externally applied uniform magnetic field, $\vec{B}$, the ball exhibits precession. A particularly intriguing observation, and a central focus of this work, is the change in precession direction when the magnetic field is reversed, while the spin of the ball remains largely unaffected.

This paper aims to provide a comprehensive theoretical explanation for such behavior, extending the analysis to include the effects of gravity. We employ the powerful Euler-Lagrange formalism, which is exceptionally well-suited for systems with constraints and for identifying conserved quantities (e.g., Goldstein et al. 2002; Taylor 2005). By constructing the Lagrangian for a symmetric top with a fixed magnetic moment in combined magnetic and gravitational fields, we derive the equations of motion from first principles. This approach allows for a clear understanding of the torques acting on the system and their influence on its complex rotational motion, including precession, nutation, and spin. We will pay particular attention to the derivation of the kinetic energy for a symmetric top in terms of Euler angles and the formulation of the potential energy arising from both magnetic and gravitational interactions. The conditions for steady precession and the implications of reversing the magnetic field will be thoroughly investigated.

joe.havens79@ku.edu

lucciana.caceres@ku.edu

2. SYSTEM DESCRIPTION AND COORDINATE SYSTEM

To accurately model the dynamics, we first define the physical system, the coordinate frames used to describe its motion, and the key assumptions underpinning our model.

2.1. *The Physical System: A Symmetric Top*

We model the rotating object as a rigid symmetric top. A symmetric top is characterized by two of its three principal moments of inertia being equal. Let the principal axes fixed in the body be denoted by x_1, x_2, x_3. The corresponding principal moments of inertia about these axes are I_1, I_2, I_3. For a symmetric top, we take $I_1 = I_2 \neq I_3$. The x_3-axis is defined as the symmetry axis of the top. This simplification is crucial as it makes the rotational kinetic energy expression more tractable and reflects the physical symmetry of objects like the cue ball in the TeachSpin experiment, assuming the internal magnet is aligned with its geometric axis. We assume the top is pivoted at a fixed point O. The center of mass (CM) of the top, with total mass M, is assumed to lie

on the symmetry (x_3) axis at a distance l from the pivot O.

2.2. *The Magnetic Dipole Moment*

The top possesses a permanent magnetic dipole moment $\vec{\mu}$. We assume that $\vec{\mu}$ is fixed in the body frame and is aligned with the symmetry axis (x_3-axis). Thus, in the body frame, $\vec{\mu} = \mu\hat{x}_3 = (0, 0, \mu)$, where μ is the magnitude of the magnetic dipole moment. This alignment is a common simplification and is consistent with the construction of many experimental setups.

2.3. *External Fields*

The top is subjected to two external fields:

1. **A uniform magnetic field**: $\vec{B}$. This field is fixed in the laboratory frame. We define the laboratory frame (X, Y, Z) such that $\vec{B}$ is directed along the positive Z-axis: $\vec{B} = B\hat{Z}$, where B is the magnitude of the magnetic field.

2. **A uniform gravitational field**: $\vec{g}$. This field is also fixed in the laboratory frame and directed along the negative Z-axis: $\vec{g} = -g\hat{Z}$, where g is the acceleration due to gravity.

2.4. *Generalized Coordinates: Euler Angles*

To describe the orientation of the body-fixed frame (x_1, x_2, x_3) relative to the space-fixed (laboratory) frame (X, Y, Z), we use a set of three Euler angles: ϕ, θ, ψ. Following the Z-x'-Z'' convention (often referred to as the x-convention, or as used by Taylor (2005)):

- θ **(Precession angle)**: The first rotation is by an angle θ about the lab Z-axis. This rotates the X, Y axes to intermediate X', Y' axes. The Z-axis remains $Z' = Z$. This angle describes the precession of the top's symmetry axis around the vertical.

- ϕ **(Nutation angle)**: The second rotation is by an angle ϕ about the new X'-axis (the line of nodes). This rotates Y', Z' to Y'', Z''. The X'-axis remains $X'' = X'$. The angle ϕ represents the inclination of the body's x_3-axis (the symmetry axis) with respect to the lab Z-axis. It is the angle between $\vec{\mu}$ (and x_3) and $\vec{B}$ (and Z).

- ψ **(Spin angle)**: The third rotation is by an angle ψ about the new Z''-axis, which is now aligned with the body's x_3-axis. This rotates X'', Y'' to the final body axes x_1, x_2. This angle describes the spin of the top about its own symmetry axis.

The angular velocities $\dot{\theta}, \dot{\phi}, \dot{\psi}$ are the generalized velocities. The components of the angular velocity $\vec{\omega}$ of the body, expressed in the body-fixed frame (x_1, x_2, x_3), are given by (Taylor 2005):

$$\omega_1 = \dot{\theta}\sin\phi\sin\psi + \dot{\phi}\cos\psi \tag{1}$$

$$\omega_2 = \dot{\theta}\sin\phi\cos\psi - \dot{\phi}\sin\psi \tag{2}$$

$$\omega_3 = \dot{\theta}\cos\phi + \dot{\psi} \tag{3}$$

2.5. *Key Assumptions and Model Idealizations*

The theoretical model developed in this paper relies on several key assumptions and idealizations:

1. **Rigid Body**: The top is treated as a perfectly rigid body, meaning the distance between any two points within it remains constant.

2. **Symmetric Top**: As stated, $I_1 = I_2$, simplifying the kinetic energy expression.

3. **Fixed Pivot**: The top rotates about a fixed point O. No translational motion of the pivot is considered.

4. **Alignment of $\vec{\mu}$**: The magnetic dipole moment $\vec{\mu}$ is assumed to be constant in magnitude and fixed along the body's symmetry (x_3) axis.

5. **Uniform Fields**: Both the magnetic field $\vec{B}$ and gravitational field $\vec{g}$ are assumed to be uniform over the spatial extent of the top.

6. **No Dissipation**: The model is conservative. Frictional forces (e.g., at the pivot) and air resistance are neglected. This implies that mechanical energy is conserved.

These assumptions allow for a tractable analytical solution. In real experimental systems, deviations from these idealizations (e.g., slight asymmetries, pivot friction, field non-uniformities) can lead to more complex behaviors or damping of the motion over time.

3. CONSTRUCTING THE LAGRANGIAN

The Lagrangian $\mathcal{L}$ for a mechanical system is defined as the difference between its kinetic energy T and its potential energy V: $\mathcal{L} = T - V$.

3.1. *Kinetic Energy of a Symmetric Top*

The rotational kinetic energy of a rigid body is $T = \frac{1}{2}(I_1\omega_1^2 + I_2\omega_2^2 + I_3\omega_3^2)$. For a symmetric top ($I_1 = I_2$), substituting Eqs. (1)-(3) yields:

$$T = \frac{1}{2}I_1(\dot{\phi}^2 + \dot{\theta}^2\sin^2\phi) + \frac{1}{2}I_3(\dot{\psi} + \dot{\theta}\cos\phi)^2 \tag{4}$$

This expression is fundamental for analyzing the dynamics of a symmetric top (cf. Goldstein et al. 2002).

3.2. *Potential Energy*

The potential energy V has magnetic (V_m) and gravitational (V_g) contributions.

3.2.1. *Magnetic Potential Energy*

$V_m = -\vec{\mu} \cdot \vec{B}$. With $\vec{\mu}$ along x_3 and $\vec{B}$ along Z, the angle between them is ϕ:

$$V_m = -\mu B \cos\phi \tag{5}$$

3.2.2. *Gravitational Potential Energy*

$V_g = Mgh_{CM}$. The CM is at l along x_3, so its height is $h_{CM} = l\cos\phi$:

$$V_g = Mgl\cos\phi \tag{6}$$

3.3. *The Full Lagrangian*

The total potential energy is $V_{total} = V_m + V_g = (-\mu B + Mgl)\cos\phi$. The Lagrangian is $\mathcal{L} = T - V_{total}$:

$$\mathcal{L} = \frac{1}{2}I_1(\dot{\phi}^2 + \dot{\theta}^2\sin^2\phi) + \frac{1}{2}I_3(\dot{\psi} + \dot{\theta}\cos\phi)^2 + (\mu B - Mgl)\cos\phi \tag{7}$$

4. DERIVATION OF THE EQUATIONS OF MOTION

The Euler-Lagrange equation for each generalized coordinate $q_i \in \{\theta, \phi, \psi\}$ is:

$$\frac{d}{dt}\left(\frac{\partial\mathcal{L}}{\partial\dot{q}_i}\right) - \frac{\partial\mathcal{L}}{\partial q_i} = 0 \tag{8}$$

4.1. *Equation for θ (Precession)*

Since $\partial\mathcal{L}/\partial\theta = 0$ (θ is cyclic), $p_\theta = \partial\mathcal{L}/\partial\dot{\theta}$ is conserved:

$$\begin{aligned} p_\theta &= I_1\dot{\theta}\sin^2\phi + I_3(\dot{\psi} + \dot{\theta}\cos\phi)\cos\phi \\ &= (I_1\sin^2\phi + I_3\cos^2\phi)\dot{\theta} + I_3\dot{\psi}\cos\phi = \text{constant} \end{aligned} \tag{9}$$

p_θ is the component of angular momentum along the lab Z-axis, L_Z.

4.2. *Equation for ψ (Spin)*

Since $\partial\mathcal{L}/\partial\psi = 0$ (ψ is cyclic), $p_\psi = \partial\mathcal{L}/\partial\dot{\psi}$ is conserved:

$$p_\psi = I_3(\dot{\psi} + \dot{\theta}\cos\phi) = \text{constant} \tag{10}$$

p_ψ is $I_3\omega_3$, the component of angular momentum along the body's x_3-axis, L_3.

4.3. *Equation for ϕ (Nutation)*

$\partial\mathcal{L}/\partial\dot{\phi} = I_1\dot{\phi}$, so $d/dt(\partial\mathcal{L}/\partial\dot{\phi}) = I_1\ddot{\phi}$.

$$\begin{aligned} \frac{\partial\mathcal{L}}{\partial\phi} &= I_1\dot{\theta}^2\sin\phi\cos\phi - I_3(\dot{\psi} + \dot{\theta}\cos\phi)\dot{\theta}\sin\phi \\ &\quad - (\mu B - Mgl)\sin\phi \end{aligned} \tag{11}$$

The Euler-Lagrange equation (Eq. 8) for ϕ is:

$$\begin{aligned} I_1\ddot{\phi} - I_1\dot{\theta}^2\sin\phi\cos\phi + I_3(\dot{\psi} + \dot{\theta}\cos\phi)\dot{\theta}\sin\phi \\ + (\mu B - Mgl)\sin\phi = 0 \end{aligned} \tag{12}$$

5. ANALYSIS OF MOTION AND CONSERVED QUANTITIES

5.1. *Conserved Momenta and Energy*

As derived in Sections 4.1 and 4.2, p_θ (Eq. 9) and p_ψ (Eq. 10) are conserved. Since the Lagrangian (Eq. 7) has no explicit time dependence and the forces derivable from the potential V_{total} are conservative (as per Section 2.5), the total mechanical energy E of the system is also conserved. The energy E is given by the Hamiltonian $H = \sum_i \dot{q}_i(\partial\mathcal{L}/\partial\dot{q}_i) - \mathcal{L}$, which simplifies to $E = T + V_{total}$:

$$\begin{aligned} E = \frac{1}{2}I_1(\dot{\phi}^2 + \dot{\theta}^2\sin^2\phi) + \frac{1}{2}I_3(\dot{\psi} + \dot{\theta}\cos\phi)^2 \\ - \mu B\cos\phi + Mgl\cos\phi = \text{constant} \end{aligned} \tag{13}$$

Thus, $\frac{dE}{dt} = 0$. If non-conservative forces like friction were present, dE/dt would be non-zero (typically negative), and the system would lose energy over time.

5.2. *Steady Precession*

Steady precession occurs when $\phi = \phi_0$ (constant), so $\dot{\phi} = 0, \ddot{\phi} = 0$. Also, $\dot{\theta} = \Omega_p$ (constant precession rate) and $\dot{\psi} = \omega_s$ (constant spin rate). The nutation equation (Eq. 12) becomes:

$$\begin{aligned} -I_1\Omega_p^2\sin\phi_0\cos\phi_0 + I_3(\omega_s + \Omega_p\cos\phi_0)\Omega_p\sin\phi_0 + \\ (\mu B - Mgl)\sin\phi_0 = 0 \end{aligned} \tag{14}$$

If $\sin\phi_0 \neq 0$ (i.e., $\phi_0 \neq 0, \pi$), we divide by $\sin\phi_0$:

$$-I_1\Omega_p^2\cos\phi_0 + I_3(\omega_s + \Omega_p\cos\phi_0)\Omega_p + (\mu B - Mgl) = 0 \tag{15}$$

Using $p_\psi = I_3(\omega_s + \Omega_p\cos\phi_0) = I_3\omega_3$ (from Eq. 10, where ω_3 is the constant angular velocity about the symmetry axis), this becomes a quadratic equation for Ω_p:

$$-I_1\Omega_p^2\cos\phi_0 + I_3\omega_3\Omega_p + (\mu B - Mgl) = 0 \tag{16}$$

For a "fast top" where $p_\psi = I_3\omega_3$ is large, such that $|I_3\omega_3\Omega_p| \gg |I_1\Omega_p^2\cos\phi_0|$, we approximate:

$$\Omega_p \approx \frac{Mgl - \mu B}{I_3\omega_3} = \frac{Mgl - \mu B}{p_\psi} \tag{17}$$

5.3. *Boundary Conditions*

The specific trajectory is determined by initial conditions: $(\phi(0), \theta(0), \psi(0))$ and $(\dot{\phi}(0), \dot{\theta}(0), \dot{\psi}(0))$. These set the values for the conserved p_θ, p_ψ, and E. For experiments like TeachSpin, a high initial $\dot{\psi}(0)$ is common, with $\dot{\phi}(0) \approx 0$ and $\dot{\theta}(0) \approx 0$.

6. EFFECT OF MAGNETIC FIELD REVERSAL

Reversing the magnetic field ($\vec{B} \to -\vec{B}$) means $B \to -B$ in our equations (assuming μ is the magnitude). The Lagrangian (Eq. 7) becomes $\mathcal{L}'$ with $(\mu(-B) - Mgl)\cos\phi = (-\mu B - Mgl)\cos\phi$. The forms of p_θ (Eq. 9) and p_ψ (Eq. 10) remain unchanged, so these quantities are conserved through an instantaneous field reversal. Consequently, $\omega_3 = p_\psi / I_3$ remains constant. The nutation equation (Eq. 12) changes:

$$I_1\ddot{\phi} - I_1\dot{\theta}^2 \sin\phi\cos\phi + I_3(\dot{\psi} + \dot{\theta}\cos\phi)\dot{\theta}\sin\phi + (-\mu B - Mgl)\sin\phi = 0 \tag{18}$$

For steady precession, Eq. (16) becomes:

$$-I_1\Omega_p^2\cos\phi_0 + I_3\omega_3\Omega_p + (-\mu B - Mgl) = 0 \tag{19}$$

The approximate precession rate (cf. Eq. 17) becomes:

$$\Omega_p' \approx \frac{Mgl - (-\mu B)}{I_3\omega_3} = \frac{Mgl + \mu B}{p_\psi} \tag{20}$$

Comparing Ω_p (Eq. 17) and Ω_p' (Eq. 20): If $|\mu B| \gg |Mgl|$ (magnetic torque dominates), then $\Omega_p \approx -\mu B/p_\psi$ and $\Omega_p' \approx \mu B/p_\psi$, so $\Omega_p' \approx -\Omega_p$, a reversal of precession direction. If $l = 0$ (pivot at CM), $Mgl = 0$, leading to $\Omega_p \approx -\mu B/p_\psi$ and a clear reversal. If $Mgl = \mu B$ (and $p_\psi > 0$), then $\Omega_p \approx 0$, and $\Omega_p' \approx 2\mu B/p_\psi$. The change in the sign or magnitude of the effective torque, proportional to $(\mu B - Mgl)$, dictates the change in precessional behavior. An example of such a reversal, observed experimentally, is shown in Figure 1. Understanding and controlling such directional changes induced by field manipulation is fundamental in various physical systems, from guiding charged particle beams to manipulating quantum spins in spintronic devices or probing astrophysical magnetic fields.

7. DISCUSSION: THE TEACHSPIN EXPERIMENT CONTEXT

The TeachSpin Magnetic Torque apparatus provides a practical realization of the system analyzed.

- **Symmetry and Alignment**: The cue ball acts as a symmetric top ($I_1 = I_2$). The embedded magnet provides $\vec{\mu}$, assumed aligned with the symmetry axis (x_3). The marker visualized in Figure 1 is typically on this axis.

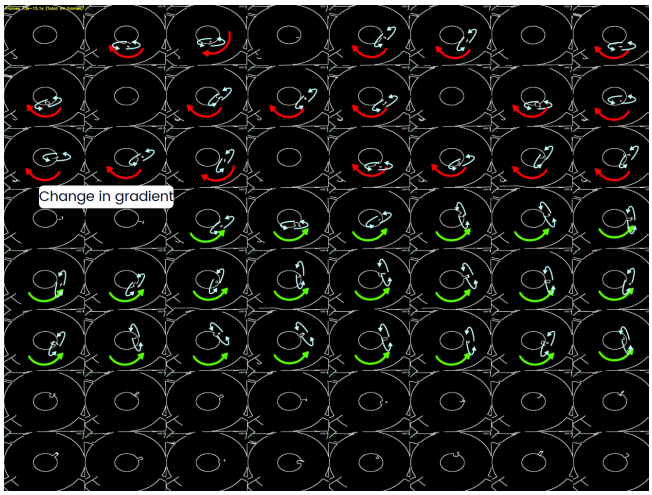

Figure 1: Experimental observation of precession reversal from a system analogous to the TeachSpin apparatus. Frame-by-frame analysis of a marker on a spinning top. Red arrows indicate the direction of precession, changing from clockwise (upper panels, $t < 13$s) to counter-clockwise (lower panels, $t > 15.1$s) after the external magnetic field is reversed (reversal occurs during $13.0\text{s} < t < 15.1\text{s}$). Light blue arrows trace the persistent elliptical path of the marker, indicative of combined spin and nutation.

- **Fast Spin**: High initial spin $\dot{\psi}(0)$ makes p_ψ large, often validating the fast top approximation (Eq. 17).

- **Field Reversal Observation**: The experiment, as illustrated by data like that in Figure 1, clearly shows precession reversal. Our analysis (Eqs. 17 and 20) attributes this to the change in the effective torque. The relative magnitudes of Mgl and μB determine the exact nature of the change.

- **Constant Spin** ω_3: Conservation of $p_\psi = I_3\omega_3$ means ω_3 is constant. If $\dot{\theta}\cos\phi$ is small (fast top, slow precession), then $\dot{\psi} \approx \omega_3$ is nearly constant.

The Lagrangian formalism effectively models this system. Quantitative comparison with experiments, especially for non-steady motion or parameter determination (μ, l), requires precise tracking of Euler angles, as discussed in Section 9.

8. CONCLUSION

We have theoretically investigated the rotational dynamics of a symmetric magnetic top in external magnetic and gravitational fields using Lagrangian mechanics. Key findings include:

1. Derivation of the Lagrangian (Eq. 7) incorporating kinetic energy (Eq. 4) and potential energies (Eqs. 5, 6).
2. Identification of conserved momenta p_θ (Eq. 9) and p_ψ (Eq. 10), and total energy E (Eq. 13).
3. Derivation of the full equations of motion, including the nutation equation (Eq. 12).
4. Analysis of steady precession (Section 5.2), yielding an approximate rate $\Omega_p \approx (Mgl - \mu B)/p_\psi$ (Eq. 17).
5. Examination of magnetic field reversal (Section 6), predicting a new precession rate $\Omega_p' \approx (Mgl + \mu B)/p_\psi$ (Eq. 20), explaining observed phenomena like that in Figure 1.

This model provides a robust framework for understanding such classical systems, highlighting the interplay of symmetries, conservation laws, and external torques.

9. FUTURE WORK AND EXPERIMENTAL VALIDATION

This model could be extended by including dissipative effects (friction, air resistance), which would cause E, p_θ, and p_ψ to decay (unofficial in-lab tests showed this took several minutes for significant decay to occur, which is why such effects were ignored in this paper). Experimental verification of the full dynamics, including nutation (partially seen in Figure 1) and dependencies on system parameters, is crucial. Advanced measurement techniques, such as computer vision systems like PYAXIOMA (Havens & Caceres Holgado 2025), are ideal for capturing detailed time-series data of $\phi(t), \theta(t), \psi(t)$. This would enable rigorous testing of the equations of motion (e.g., Eq. 12) beyond steady precession and aid in accurate parameter determination (I_1, I_3, μ, l), refining our understanding of the system and the limits of the ideal model.

ACKNOWLEDGMENTS

We sincerely thank the University of Kansas for providing the TeachSpin Magnetic Torque apparatus, and Jessy Changstrom and Cole Douglas Le Mahieu for their support. This work builds upon methods in texts like Taylor (2005) and Goldstein et al. (2002).

REFERENCES

Goldstein, H., Poole, C. P., Jr., & Safko, J. L. 2002, Classical Mechanics, 3rd edn. (Addison-Wesley, San Francisco, CA)

Havens, J., & Caceres Holgado, L. M. 2025, Proposed Methodology for Non-Contact Angular Measurement via Computer Vision - PYAXIOMA-JH, unpublished manuscript, Department of Physics and Astronomy, University of Kansas

Taylor, J. R. 2005, Classical Mechanics (University Science Books, Sausalito, CA)